Phys Chem Minerals (2003) 30: 373–381
DOI 10.1007/s00269-003-0327-1
© Springer-Verlag 2003

ORIGINAL PAPER

A. A. Finch · D. E. Hole · P. D. Townsend

Orientation dependence of luminescence in plagioclase

Received: 31 October 2002 / Accepted: 12 April 2003

Abstract The orientation dependence of the luminescence of a well-characterized plagioclase crystal at room temperature and 40 K is reported. A beam of H^+ ions was used to provide the excitation. Ion beam luminescence provides emissions effectively from the bulk of the material, and therefore minimizes the contribution to the luminescence from atypical regions. The intensity of the luminescence is strongly orientation-dependent. The intensity and photon energy, particularly of the red/infrared and yellow emission bands, vary significantly. We interpreted this as resulting from Fe^{3+} and Mn^{2+} activator ions, respectively, on crystallographic sites with low point symmetry. An emission at 860 nm was also significantly orientation-dependent. The blue luminescence showed the least variability. At room temperature, a 350 nm near-UV emission was noted, whereas at 40 K, emissions were at 240, 260, 300 and 340 nm. UV emissions may result from Na^+ diffusion along interfaces within the plagioclase, notably albite-law (010) twins. This variability has significant consequences for the use of single-crystal quantitative luminescence techniques. We have also studied the dependence of the peak intensities and profiles during prolonged ion beam bombardment with heavier (He^+) ions. Broadening of the red-infrared emission is interpreted as reflecting growing amorphization of the sample.

Keywords Feldspar · Ionoluminescence · Ion beam luminescence

A. A. Finch (✉)
Centre for Advanced Materials and School of Geography & Geosciences, University of St Andrews, Irvine Building, St Andrews, Fife KY16 9AL, UK
e-mail: aaf1@st-and.ac.uk

D. E. Hole · P. D. Townsend
School of Engineering & Information Technology, University of Sussex, Pevensey Building, Brighton, Sussex, BN1 9QH, UK

Introduction

Luminescence is light emission when energy is deposited into a material. The means of delivering energy can be divided into two broad types: stimulation, where the magnitude of the incident energy is less than that of the emitted light, and excitation, when the incident energy is greater. Forms of stimulation include heat (thermoluminescence, TL) and laser light (optically stimulated luminescence, OSL); excitation includes electron beam irradiation (cathodoluminescence, CL) or X-irradiation (radioluminescence, RL). Whatever the nature of the incident energy, the energy cascades associated with the subsequent luminescence are often similar, and hence different forms of excitation/stimulation explore subtly different aspects of luminescence centres within materials. Many minerals are luminescent, and applying these signals to solve geological problems is an important and expanding field. For example, OSL and TL of framework silicates are the basis for luminescence dating of Quaternary sediments, and CL petrography is a widespread mineral-prospecting tool.

In low-symmetry materials, structural anisotropy causes the physical properties of a crystal to be orientation-dependent. Such dependence within individual grains is often ignored when studying fine-grained rocks or powders, in which many crystals are randomly oriented, and the response is therefore averaged over all possible orientations. However, studies of single grains of anisotropic minerals or rocks with fabrics (in which minerals are aligned) will demonstrate orientation dependence. Feldspar, the subject of the present study, has monoclinic or triclinic symmetry, with the result that the physical properties of the crystal are independent in all three dimensions. For that reason, the luminescence of feldspar single grains will depend (to some degree) on orientation of the crystal. Changes in luminescence as a function of orientation can also provide insights into the nature and origins of luminescence centres.

The present study examines how the intensity and photon energy of the major emission bands change normal to each of the {100} form faces. We measure the orientation dependence of the luminescence of a well-characterized plagioclase (AF/96/4), which demonstrates all four major luminescence bands found in feldspar perpendicular to (100), (010) and (001) faces. Analysis of this sample allows us to examine simultaneously the orientation dependence of the major emission bands in feldspar.

Choice of incident energy

Excitation/stimulation for light-emission studies can be achieved by a variety of routes. For studying all luminescence centres in solids, excitation with high incident power density is employed, and, for ease of analysis, the primary excitation needs to be a focused, parallel beam. This rules out many forms of incident energy, since TL and OSL, for example have low power densities, and conventional RL uses an unfocused source. Cathodoluminescence (CL) is a widely used method whereby an electron beam excites the sample. Because electrons are charged, the beam can be focused and, by increasing the acceleration potential and current, large incident power densities (e.g. 10^2 W m^{-2}) can be achieved. However, the majority of the energy from electrons is deposited within the outermost submicron-thick layer of the sample, providing only luminescence characteristic of the surface region. Comparisons of RL and CL responses in alkali feldspars (Brooks et al. 2002) have shown that feldspar surfaces provide luminescence that is highly atypical of the bulk. For anisotropic media, such as feldspar, the nature of the surface is likely to be orientation-dependent.

Recently, experiments have been performed using ion beams as an excitation source for luminescence (ionoluminescence, IL, or ion beam luminescence, IBL). Ion beams have high incident power densities, and can be focused to analytical spots typically of areas of mm^2 or less. Ion beams effectively penetrate the sample bulk to, e.g., tens of μm depths in contrast to CL, in which the incident beam is stopped within a few nm of the surface and provides a surface-dominated response. For H^+ or He^+ ions at MeV energies (the conditions used in the present study, see below), $>90\%$ of the incident energy is deposited fairly evenly as electronic excitation along the ion track. At the end of the track (e.g. in a ~1-μm width zone), nuclear collision accounts for the remaining $<10\%$ of the energy. Most of that energy is dissipated in the form of atomic displacements, which give rise to thermal rather than electronic processes, and therefore contributes relatively little to the overall luminescence. Therefore relatively little of the IL signal derives from regions atypical of the bulk, either at the surface or at the end of the track. IL is therefore an important form of excitation for luminescence studies, since it is high-energy, focusable, and provides a response dominantly from the bulk. Homman et al. (1995) first performed IL on plagioclase and, more recently, Brooks et al. (2002) compared RL, IL and CL responses from microperthitic alkali feldspar, comparing and contrasting the three excitation methods. IL is particularly appropriate for understanding the orientation dependence of luminescence, the focus of the present study. A disadvantage of IL is that some sample degradation results from the ion beam interaction. The sample undergoes structural damage particularly at the end of the ion track, and this can modify the sample, particularly when using heavy ions at high acceleration potentials and high beam currents. However, light ions (such as H^+) at moderate incident power densities (e.g. 10^4 W m^{-2}) cause little sample degradation in feldspar over the time-scales of the experiments described below (< 10 h). Note also that sample damage and modification also occur with other forms of excitation, particularly CL.

Material studied

The sample studied (AF/96/4) is a cleavage fragment from a remarkable 1 m^3 plagioclase megacryst, part of an exceptionally coarse gabbro unit in the Klokken centre, Gardar Province, South Greenland. Parsons (1979, 1981) gives descriptions of the geological context of the unit, and Emeleus and Upton (1976), Upton and Emeleus (1987) and Upton et al. (2003) review Gardar geology as a whole. The Klokken intrusion has been dated at 1166.6 ± 1.2 Ma (Burgess et al. 1992). The plagioclase was sampled as cleavage fragments ~15 × 10 × 10 in size, from which small fragments (e.g. 0.5 × 0.5 × 0.5 cm) were broken in the lab. The plagioclase is dark bottle green in hand specimen with obvious repeated (010) twinning. In thin section, the feldspar is perfectly transparent (pristine) with little evidence for late-stage hydrothermal alteration. It has a nominal composition $\sim An_{51}Ab_{45}Or_4$ determined by X-ray fluorescence, but the feldspar contains small inclusions of magnetite, olivine, biotite and apatite (Hobbs 1999), and these (particularly biotite mica) may have exaggerated the apparent Or component. By X-ray diffraction the sample conforms to the pattern of a triclinic, ordered intermediate plagioclase. However, the μm-scale multiple (010, albite) twinning gives the sample an effectively monoclinic symmetry when analyzed on the mm scale (as in the present study), since at this scale the responses of the left-and right-handed triclinic twin domains are averaged. Electron diffraction using the transmission electron microscope shows pairs of *e* diffraction spots typical of intermediate plagioclase. Additional weak *f* satellites are observed around *a* diffraction spots. The composition is close to the solvus of the Bøggild intergrowth, but there is no evidence for Bøggild-type intergrowths in TEM images, and there is no Schiller effect (indicative of intergrowths of the size of the wavelength of light) in hand specimen. There are, however, occasional thin disc-like precipitates 10–40 nm long and ~2 nm wide, which may be exsolved K-feldspar (M.A. Carpenter, personal communication, 1998). AF/96/4 is therefore a relatively K-rich e_2-plagioclase.

Analytical methods

IL investigations were carried out under vacuum using the 3 MeV Van der Graaf accelerator facility at the University of Sussex generating a spot size of ~0.25 cm^2. For investigations of temperature dependence, a proton beam at 0.95 MeV generated the luminescence with an ion current of ~100 nA. The beam generated

an incident power density of ~2 kW m^{-2}. H^+ ions were used to minimize the collision damage caused to the sample. IL data were collected every 10 K between 40 and 160 K and then at 20 K intervals up to 300 K. Cryogenic temperatures were achieved using an 8 W He compressor, and thermal contact between the compressor head and the sample was maintained using Ag dag. Under the conditions outlined above, the incident beam deposits < 0.1 W of power, and analysis of standard materials with strong temperature dependence do not show significant (e.g. < 5 K) heating at the sample surface. When ramping the temperature, the sample was irradiated only whilst data were being acquired, to reduce the exposure. A typical ion dose during an experimental run was $\sim 5 \times 10^{15} H^+$ ions. Repeat analyses of the same samples show excellent reproducibility in the luminescence profiles, although differences in the positioning and size of different samples (i.e. the way in which the position is optimized with respect to the system optics) causes some variation in intensity. IL analysis was performed on freshly exposed feldspar cleavage surfaces for (010) and (001) and a fracture surface for the (100) face — the morphology of the cleavage fragments allows the orientations to be identified unambiguously. The results are the averages of typically three runs on each face. Ideally, we seek to arrange the primary beam and the secondary optics exactly normal to the crystal surface, but such a geometry would cause interaction between the primary beam and the earthed secondary optical system. We therefore oriented the sample such that the ion beam encounters the surface of the sample at an angle of ~22° from the normal to the sample face, and the light is collected 22° from the perpendicular in the opposite direction. The incident beam and the emitted light vary by 45°. Such a geometry allows both the incident beam and emitted light to be close to perpendicular with respect to the sample, whilst also ensuring that the primary beam and light collection system do not interfere. A goniometer was not used. Using a standard modelling package, this geometry gives an estimated penetration range of the H^+ ions into silica as ~10 μm. Light emissions were collected by a quartz fibre optic coupled to a f/4 SpectroPro 300i monochromator. The detector used was a Roper Scientific image intensified CCD camera operated using the WinSpec software package. The system operates in the range 200–1100 nm by performing two separate spectral analyses between 200 and 600 and 500 and 1100 nm, respectively, and then matching the spectra in the 500–600 nm region. Raw intensity counts were typically integrated to > 10 000 for the brightest peak, compared with a background of ~200 counts. The intensity data were corrected for system response against a W lamp by assuming a black-body radiation profile. Wavelength was calibrated against the emissions of an Hg lamp and the resolution at the analytical conditions applied corresponded to ~2 nm. Sample degradation experiments were carried out on the (001) face at room temperature, using 2 MeV $^4He^+$ ions. Beam currents were ramped between 50, 1000 and 2500 nA to allow a range of integral ion doses between 10^{13} and 10^{17} ions over time periods of hours.

Feldspars have been known for several decades to emit light when excited (e.g. Smith and Stenstrom 1965). The prominent luminescence bands observed in feldspars, their nature and probably causes are given in Table 1. In addition to the prominent bands, Brooks et al. (2002) reported a minor orange band at ~620 nm that they identified as a defect-related structure. Preliminary CL analysis showed AF/96/4 demonstrates four major luminescence bands in the red/IR, yellow, blue and near UV spectral regions. Finch and Klein (1999), Götze et al. (2000) and Brooks et al. (2002) give further summaries of feldspar luminescence.

Results and discussion

Sample degradation during H^+ analysis

Ion beam implantation can cause some sample degradation. Brooks et al. (2002) showed that degradation was observed in alkali feldspars, particularly after prolonged implantation with He^+ ions, but that degradation with H^+ was very slow. In order to monitor sample damage, we performed comparable IL runs at room temperature before and after the IL experiments. Figure 1 shows the emission from the (010) cleavage face before and after implantation by ~10^{17} H^+ ions. Note that this dose is greater than that experienced by samples in the present study (~4×10^{15} ions). The sample does show subtle changes in the relative intensities of the emissions as a result of the implantation. The greatest change is observed around 750 nm, in which there is a reduction in intensity during irradiation by < 10%. If the sample is allowed to recover for 18 h, there is no modification of the spectrum. Similar responses are observed for the beam dependence of other orientations. IL therefore does show some minor modification of the sample during implantation, but this is very small, particularly in comparison with the orientation dependence at the heart of the present study. It is important to note that such modification is also observed using other forms of excitation, such as CL. We conclude that IL provides conditions with stabilities as a function of time that are comparable to, or better than, other forms of excitation.

Light emission at room temperature

The luminescence response at room temperature shows broad bands in the red/IR (700–820 nm), yellow (~560 nm) and blue (~420 nm) spectral regions with evidence for emission in the UV (~350 nm) (Fig. 2a). Table 2 provides estimates of the peak positions and intensities as a function of temperature and sample orientation. The red/IR peak is the most intense, and the asymmetry of that band provides evidence for an extra emission on the long-wavelength side of the IR peak, with a maximum at ~860 nm. In addition, there is a

Table 1 Summary of major feldspar luminescence bands and possible origins

Band	Wavelength /nm	Energy /eV	Possible origin	Reference
UV	280	4.42	Strain and/or ionic diffusion	Garcia–Guinea et al. (1999)
UV	350	3.54	Strain and/or ionic diffusion	Garcia–Guinea et al. (1999)
Blue	400–450	3.00–2.75	O Paramagnetic defect Eu^{2+} activation	Finch and Klein (1999) Götze et al. (1999)
Yellow	580	2.14	Mn^{2+} activation	Telfer and Walker 1976)
Red/IR	750	1.65	Fe^{3+} activation	Brooks et al. (2002)

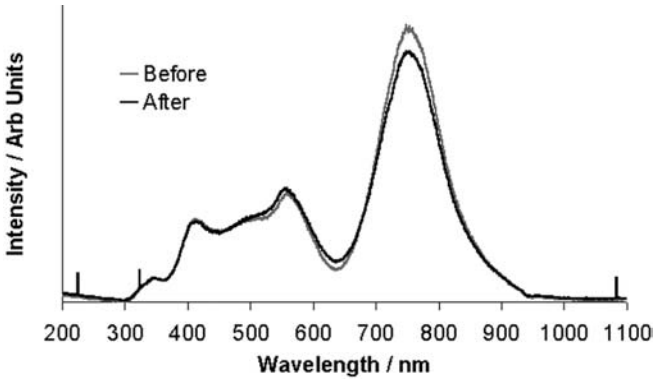

Fig. 1 Comparison of the IL spectra perpendicular to the (010) face before and after the ion beam experiment. Note that there are subtle differences in the spectra caused by the implantation, but these are small compared with the changes discussed in the text as a function of orientation and temperature. The sample modification is typical of all the orientations

small emission band at ~500 nm. Figures 2 and 3 show the luminescence normal to the three {100} form faces at room temperature and 40 K, respectively. The first diagram in each shows the intensity as a function of wavelength, the second the log(intensity) as a function of photon energy. Differences between the intensities and peak positions of many emissions are observed. For example, in the room-temperature spectra (Fig. 2), a shift in the peak position of the red/IR emission is present as the orientation is changed. Whereas normal to the (001) face the maximum of this broad band occurs at ~757 nm, it occurs at ~765 nm for the other two. In addition, differences in the position of the ~555 nm peak are evident. Perpendicular to the (100) plane, the peak position has shifted to shorter wavelengths (~550 nm). Differences between the emissions in the blue and UV regions are most obvious in a graph of the

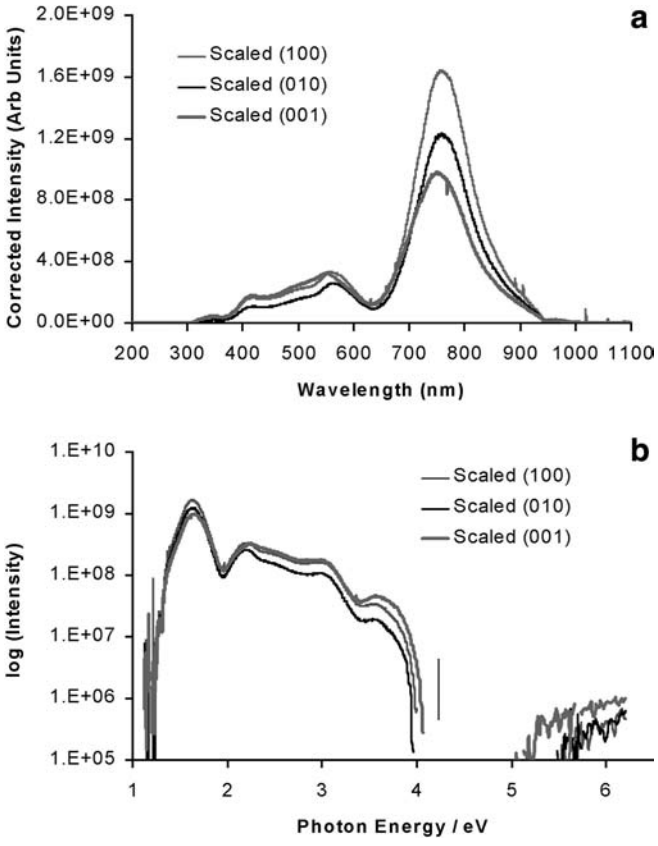

Fig. 2a The luminescence spectra normal to the three {100} form faces as corrected intensity versus wavelength for samples at room temperature. **b** Representation of the data in **a** (room temperature), presented as log(corrected intensity) versus photon energy

photon energy versus log(corrected intensity) (Figs. 2b, 3b). Note that near-UV luminescence (~3.53 eV, ~350 nm) is evident.

Table 2 Summary of the luminescence emissions observed in AF/96/4 as a function of orientation and temperature

Temperature	Peak position	Peak intensity	Comments
Room temperature	350 nm 3.53 eV	$\sim 3 \times 10^{7}$	All faces
	415 nm 2.99 eV	1.6×10^{8}	All faces
	~550 nm 2.25 eV	3.2×10^{8}	(001) face
	~560 nm 2.21 eV	3.3×10^{8}	(100) face
	~560 nm 2.21 eV	2.6×10^{8}	(010) face
	757 nm 1.64 eV	1.0×10^{9}	(001) face
	765 nm 1.62 eV	1.6×10^{9}	(100) face
	765 nm 1.62 eV	1.2×10^{9}	(010) face
	~860 nm 1.44 eV	$\sim 4 \times 10^{8}$	Small peak — difficult to resolve exact energies and intensities
40 K	240 nm 5.16 eV	8×10^{6}	Strongest from (001) face
	260 nm 4.76 eV	4×10^{6}	Strongest from (001) face
	300 nm 4.14 eV	8×10^{6}	Strongest from (001) face
	340 nm 3.61 eV	5×10^{7}	All faces
	415 nm 2.99 eV	1.2×10^{8}	All faces
	500 nm 2.48 eV	1.4×10^{8}	All faces
	568 nm 2.18 eV	1.3×10^{8}	(100) face
	570 nm 2.17 eV	7×10^{7}	(010) face
	782 nm 1.58 eV	3.3×10^{9}	(100) face
	790 nm 1.57 eV	3.0×10^{9}	(001) face
	790 nm 1.57 eV	2.2×10^{9}	(010) face
	~910 nm 1.36 eV	$\sim 6 \times 10^{8}$	All faces

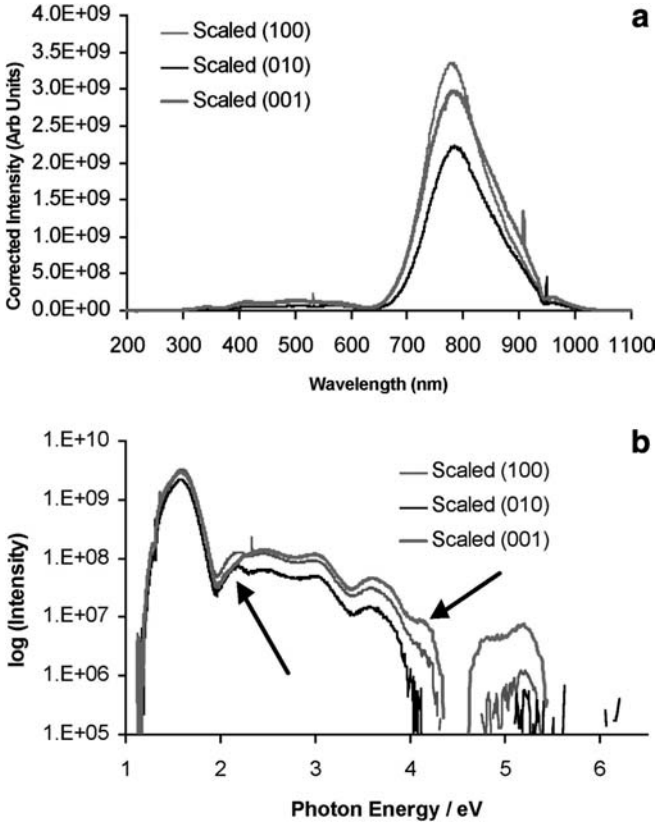

Fig. 3a The luminescence spectra normal to the three {100} form faces as corrected intensity versus wavelength for samples at 40 K. **b** Representation of the data in **a** (40 K), presented as log(corrected intensity) versus photon energy. *Arrows* identify features at 2.2 and 4.2 eV that are different for the (001) data

Light emission at 40 K

The analysis at 40 K (Fig. 3) bears many similarities to the data at room temperature. The red/IR emission is over double the intensity, accompanied by an energy shift, moving from ~1.62 to ~1.57 eV as the temperature falls. Similarly, the IR shoulder to the peak at ~1.44 eV (860 nm) moves to ~1.36 eV (~910 nm). There are subtle changes to peak positions in the yellow (2.17 eV) region, whereas the blue emission appears little changed in energy (3.0 eV). Figure 3b shows the log(intensity) as a function of photon energy, and is particularly useful in showing detail in the near-UV. Emissions at ~4.14, 4.76 and 5.16 eV (corresponding to ~300, 260 and 240 nm, respectively) are absent at room temperature (Fig. 2b), but present at 40 K (Fig. 3b) and particularly strong perpendicular to the (001) face.

The luminescence as a function of orientation is markedly different at both temperatures. The red/infrared emission at 40 K varies in intensity by ~30% between the faces analyzed, with the emission weakest normal to the (010) face; some small shifts in the peak position may also occur. This is a smaller variation than observed at room temperature. There are also changes in the intensity and position of yellow and UV bands. The orientation dependence appears least marked in the blue.

Detailed analysis of the intensities of luminescence from the three planes is more complex. Variations in sample size and positioning in the sample holder introduce variability into the intensities of light recorded, and so comparisons of absolute emission intensities are difficult. The profiles of the luminescence normal to the (100) and (010) faces are similar and can be broadly matched by magnifying the raw (010) counts by ~30%. The data perpendicular to these faces, therefore, although they have different intensities, have near-identical profiles. In contrast, the profile normal to the (001) face is quite different. No scaling of the (001) profile allows it to be matched with the response from either of the other planes.

Ion beam dose dependence

We examined the dependence of luminescence of one feldspar face, (001), to ion beam degradation at room temperature. Brooks et al. (2002) first performed this type of experiment on feldspar, examining microperthitic alkali feldspar. We present here a description of the ion beam degradation of the AF/96/4 plagioclase. Briefly, the dependence of luminescence as a function of ion beam interaction allows important insights into the nature of luminescence centres and their stability to high-energy electronic and structural modification. Note that for these experiments, we used heavier ions (He^+) at much greater incident power densities than in the temperature dependence studies above.

We have considered the intensity of the IR, yellow, blue and 350 nm UV bands as a function of implantation dose (Fig. 4). Luminescence intensity falls as the implantation progresses for all the emission bands. In addition, there are inflexions in the intensity (labelled A and B, Fig. 4) which correspond to the points during the experiment at which the ion beam current was increased. So that the total implantation dose can be achieved within convenient time scales, we performed the experiments at three beam currents, 50 nA, 1 μA and 2.5 μA. The points A and B (Fig. 4) correspond to the doses at which the current was increased. These changes demonstrate that the sample is responding not only to the total number of ions implanted, but also to the implantation dose rate. For all but the red/infrared band, the change from 50 nA to 1 μA is associated with a jump in the luminescence, whereas at the highest beam current there is a notable drop for all the emission bands. This is similar to the behaviour of the red/IR band observed in microperthite by Brooks et al. (2002). Brooks et al. considered the possible interpretations of this dose-dependent behaviour in feldspar. A key idea presented by these authors was that at higher dose rates, there was an increased probability of ions arriving close together in time and space, forming aggregate defect structures that develop at the expense of the single ion

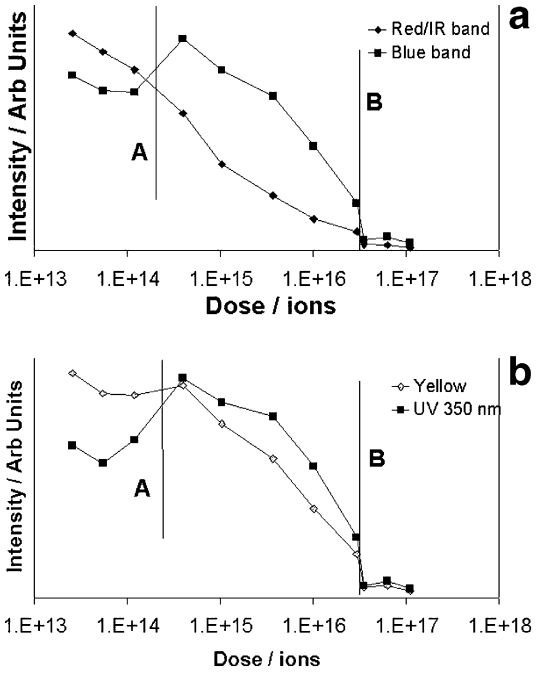

Fig. 4 Dose dependence of the four main luminescence bands at room temperature. The blue and red emissions are shown in **a**, the yellow and UV bands in **b**. The *lines marked A and B* mark the points at which the ion current was increased from 50 to 200 nA (*A*) and 200 nA to 1 μA (*B*)

luminescence centres. Such behaviour would be most likely for luminescence cascades with long decay times. In the study of AF/96/4, we observe that the dose rate dependence is strongest in the UV 350 nm and blue emissions, but less marked for the red and yellow emissions (Fig. 4). The decay time of the blue emission in feldspar is relatively short (e.g. 6 μs, Finch and Klein 1999), whereas those of the yellow and red/infrared bands are orders of magnitude longer (e.g. 2 ms, Finch and Klein 1999). If that model for the dose-rate dependence were correct, then the clearest dose-dependent effects would be observed for the red and yellow bands, with the longest decay times. This is not the case. We therefore attribute the dose-dependent behaviour reported here and by Brooks et al. (2002) to a combination of sample charging (deflecting the incoming beam) and heating. At the highest currents, the incident beam deposits a power density of ~0.1 MW m^{-2}. In contrast to studies at smaller currents, analysis at 2.5 μA caused significant sample heating. A thermocouple immediately next to the sample showed heating by ~10 K during experiments at high currents. The dose-rate dependence of feldspars is the subject of future study (A. A. Finch, personal communication).

In addition to variability in the intensities of the emissions, there are changes in the peak profiles. We observe that the red/IR emission becomes asymmetrical and moves to shorter wavelengths during the implantation (Fig. 5). This is similar to behaviour reported by Brooks et al. (2002), who explained this peak shift in terms of changes to the coordination sphere of the

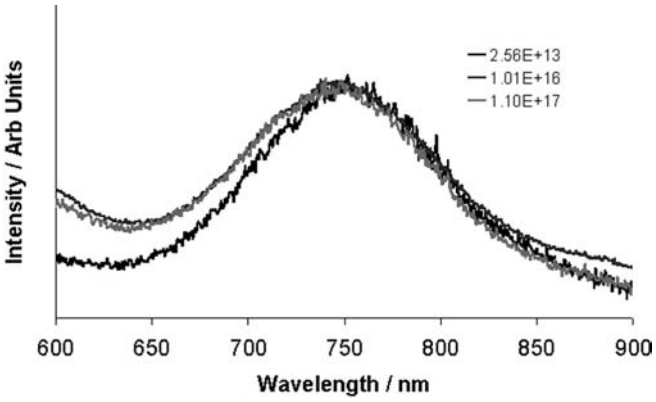

Fig. 5 The dose dependence of the profile of the red/infrared emission as a function of integral dose. The profile shifts towards the red/orange regions during implantation, but the shift is complete by 10^{16} ions

activator Fe^{3+} ion caused by the ion bombardment. Comparison of the profiles at 1×10^{16} and 1×10^{17} ions shows no change in the luminescence profile, demonstrating that the local structural modification is largely complete by 10^{16} ions. The ~850 nm band reduces in intensity with dose, apparently linearly with the ~750 nm band, suggesting that the luminescence centres causing these bands have common features. However, it is impossible to resolve any developing asymmetry in the ~850 nm emission (as might be expected by analogy with the ~750 nm emission), given its proximity to the dominant IR band.

Discussion

The orientation dependence of particular emissions provides insights into the nature of the luminescence centres, particularly when this is coupled with analyses at room and cryogenic temperatures. Centres with high point symmetries will give little orientation dependence, whereas those in low symmetry sites will give emission energies and intensities that are significantly different as the crystal is rotated. In addition, the variation in band energy, intensity and orientation dependence as temperature is changed also provides insights into the way in which the luminescence cascade couples with the mineral lattice. We interpret below the observed orientation dependence in each of the four major emission bands.

UV luminescence

UV TL emissions at 290 and 340 nm were reported in alkali feldspars by Garcia–Guinea et al. (1999). Na^{+} ions in albites (as high, low and mon-albite) have highly anisotropic thermal displacement ellipsoids at room and cryogenic temperatures (Previtt et al. 1976; Harlow and Brown 1980; Smith and Artioli 1986; Armbruster et al. 1990). Garcia–Guinea et al. (1999)

suggested that thermally assisted Na^+ ionic diffusion, predominantly along (010) planes, was responsible for the 290 nm emission. They also attributed the 340 nm emission to $[AlO_4]^\circ$ centres on the feldspar framework. Our data differ somewhat from their observations. We note a 350 nm (3.53 eV) emission, significantly offset from 340 nm. The contrasting composition between the alkali feldspars studied by Garcia–Guinea et al. and the plagioclase of the present study may explain the decreases in the emission energy of this feature. Interatomic distances in $An_{50}Ab_{50}$ plagioclase are smaller than in alkali feldspars, and thermally assisted ionic diffusion will therefore occur at lower energies. However, we observe little significant orientation dependence in the emission at room temperature, in contrast to Garcia–Guinea et al. (1999).

The majority of features in the near-UV are apparent at 40 K. Small but significant peaks occur at 240, 260, 300 and 340 nm (5.16, 4.76, 4.14 and 3.61 eV, respectively); (Fig. 3b). The first three emissions are particularly strong normal to the (001) face, whereas the 340 nm emission appears less orientation-dependent. The 340 nm emission at 40 K may be analogous to the 350 nm band at room temperature, and the energy shift would indicate a luminescence centre coupled to lattice vibrations and/or interatomic distances. Alternatively, the two emissions may derive from different centres, in which case, the latter may equate to the 340 nm emission of Garcia–Guinea et al. (1999). The exact origins and complexity of the UV emissions remain problematic. Garcia–Guinea et al. considered ionic diffusion along surfaces or interfacial boundaries to be responsible for the emission. Loss of singly charged ions caused the development of $[AlO_4]^\circ$-type centres. Highly strained interfacial states are unrepresentative of the bulk, and they may provide atypical luminescence, the understanding and determination of which are extremely difficult. AF/96/4 is similar to the majority of plagioclases in having repeated polysynthetic twinning according to the (010) albite twin law. The near-UV emissions are weakest in the (010) orientation. The orientation dependence of the low-temperature UV emissions suggests coupling with an anisotropic feature of the structure. Both the (100) and (001) orientations provide luminescence from significant numbers of albite twin planes, whereas (010)-oriented excitation would not encounter significant numbers of twin planes at the penetration depth of the ion beam. This is consistent with the observed orientation dependence of the luminescence. In addition, AF/96/4 contains small submicroscopic K-feldspar inclusions observed using TEM. These may provide alternative loci for the development of strain-related luminescence. UV emissions in feldspars are highly complex but it is clear they are related to luminescence associated with interfaces. These are highly anisotropic features of the feldspar structure which give rise to luminescence with notable orientation and temperature dependence.

Blue luminescence

The blue emission in feldspars has been linked both to Eu^{2+} activation (Götze et al. 1999) and a paramagnetic oxygen defect on the tetrahedral silicate framework (e.g. Finch and Klein 1999). Blue luminescence is common to the majority of framework silicates and paramagnetic oxygen is the dominant luminescence centre in the majority of rock-forming feldspars. Unlike yellow and red/IR emissions, the photon energy of the blue emission is unchanged as a function of temperature, occurring at $\sim$3.00 eV at both 40 K and room temperature. The overall intensity changes from room temperature to 40 K, but the intensity from each face is broadly similar. This is consistent with a centre unrelated to an activator ion on a specific crystallographic site, but rather a centre with a defect-related origin.

Yellow luminescence

Light emission in feldspars between 540 and 570 nm (the yellow-green spectral region) is linked to the presence of Mn^{2+} ions substituting for Ca^{2+} (Telfer and Walker 1976). Because of its exchange for Ca, yellow luminescence is most commonly observed in plagioclase. Götze et al. (2000) reported a linear relationship between Mn content and luminescence intensity. This luminescence band has clear orientation dependence (Figs. 2, 3), with both the peak position and intensity changing. The yellow emission is brightest normal to the (100) face at both room temperature and 40 K. The emission was not detected perpendicular to the (001) face at 40 K. Luminescence anisotropy in the yellow emission behaviour has been inferred for some time, since (010) polysynthetic (albite) twinning is readily visible in yellow luminescent plagioclases using CL petrography. No correlation between photon energy in the yellow region and plagioclase composition is reported (Götze et al. 2000) and this may be, at least in part, a consequence of the four non-equivalent crystallographic sites in which Mn^{2+} can reside. We observe that the energy and intensities of the yellow emission are decreased at low temperatures (Figs. 2, 3). Decreases in photon energy with cooling follow shrinkage of the unit cell and therefore indicate a broad correlation with the interatomic bond distances, in particular crystallographic sites. Such observations suggest that the complexity in the reported intensity and photon energy of the yellow-green emission in the literature results from samples of different compositions showing different degrees of Mn order, coupled with the orientation dependence of this band.

Red/IR luminescence

Our data extend to 1100 nm and provide a full profile of both the near and far sides of the red/IR peak. Red/IR

emissions in feldspars are believed to relate to Fe^{3+} substituting for Al^{3+} on the feldspar framework. Geake and Walker (1975) and White et al. (1986) identify the emission as a result of the $^4T_1$ to $^6A_1$ transition of tetrahedral Fe^{3+}. Some authors (e.g. Rae and Chambers 1988) have commented that there appears little correlation between the intensity of the red peak and the amount of Fe determined by electron probe microanalysis (EPMA) or secondary ion mass spectrometry (SIMS). This may result (at least in part) from the presence of submicroscopic inclusions of iron oxides within feldspars, which influence microanalysis but do not contribute to luminescence. Note also that pairing, clustering or precipitation of impurities can all reduce luminescence efficiency. Finch and Klein (1999) studied the decay times and profiles of red/IR CL of a microperthite. They showed that the decay time of the red emission in these feldspars could only be modelled successfully by the superposition of two or more different emissions, and demonstrated shifts in the peak positions between samples. In detail, the variation in the peak profiles and energies of the red/IR emission may relate to the presence of Fe^{3+} across crystallographically inequivalent sites (Finch and Klein 1999; Brooks et al. 2002). In plagioclases, red/IR emissions are reported to vary from ~745 to 690 nm as a function of anorthite content (Götze et al. 2000; Krbetschek et al. 2002). AF/96/4, with a composition in the middle of the plagioclase series, might be expected therefore to have an emission at ~720 nm. However, the red/IR maximum in our data (~755 nm) is beyond even the range of the most An-rich feldspars quoted by Götze et al. (2000).

The peak profile in energy (Figs. 2b and 3b), which is normally Gaussian for a single emission band, is skewed to the low-energy side for the IR emission in AF/96/4, reflecting the presence of a second band at lower energy. Krbetschek et al. (2002) and Götze et al. (2000) both reported an emission ~850 nm in potassium feldspars (adularia, orthoclase and microcline) which corresponds well to our observations, although that emission is not previously reported from plagioclase. Those authors were unable to assign a specific defect centre to the band.

Implications for quantitative luminescence studies

The present study identifies significant orientation dependence in the intensity and (for some emissions) photon energy of the luminescence. For example, the intensity of the IR band varies by 60% depending on orientation at room temperature, and small shifts in peak position are also observed. Quantitative methods that utilize luminescence in single grains of low-symmetry minerals must accommodate orientation dependence. For example, Habermann (2002) proposed that quantitative CL might be used as a chemical analytical tool with precision and limit of detection equivalent to particle-induced X-ray emission (PIXE). Habermann illustrated this suggestion with studies of the yellow emission of plagioclase as an indicator of Mn contents, an emission we demonstrate here as having significant orientation dependence. The precision of such analysis would be highly dependent on knowing, and being able to accommodate, the orientation of the crystal. In addition, quantitative analysis of OSL and TL is used for dating of Quaternary sediments and archaeological artefacts. Such studies are normally carried out on aliquots of samples containing significant numbers of grains. However, in recent years, the development of single-grain OSL readers has allowed luminescence studies to be performed on individual crystals. In principle, anisotropy of the luminescence response, if significant, might strongly influence the luminescence measured from grains lying in a variety of random orientations. Even assuming that orientation does not affect the regeneration doses (something that remains to be determined), certain orientations would provide brighter luminescence and therefore more precise age estimates. Precision in dating might be enhanced by rotating the single crystals into particular orientations before TL or OSL analysis. Anisotropy in low-symmetry minerals is clearly a problem that must be addressed fully for highly precise measurements of the luminescence properties of single crystals to be achieved.

Acknowledgements The present work was supported by NERC. A.A.F. acknowledges tenureship of a BP/Royal Society of Edinburgh Fellowship. Michael Carpenter (University of Cambridge) is thanked for assistance with the TEM characterization of AF/96/4. The Carnegie Trust for the Universities of Scotland and the Percy Sladen Trust have contributed to the costs of fieldwork in Greenland. The manuscript has benefited from the reviews of Karl Malmqvist and two anonymous reviewers.

References

Armbruster TH, Burgi HB, Kunz M (1990) Variation of displacement parameters in structure refinements of low albite. Am Mineral 75: 135–140

Brooks RJ, Finch AA, Hole DE, Townsend PD, Wu Z-L (2002) The red to near-infrared luminescence in alkali feldspar. Contrib Mineral Petrol 143: 484–494

Burgess R, Kelley SP, Parsons I, Walker FDL, Worden RH (1992) Ar^{40}–Ar^{39} analysis of perthite microtextures and fluid inclusions in alkali feldspars from the Klokken syenite, south Greenland. Earth Planet Sci Lett 109: 147–167

Emeleus CH, Upton BGJ (1976) The Gardar Province of South Greenland. In: Escher A, Watt WS (eds) Geology of Greenland. Grønlands Geologiske Undersøgelse, Copenhagen: pp 152–181

Finch AA, Klein J (1999) The causes and petrological significance of cathodoluminescence emissions from alkali feldspars. Contrib Mineral Petrol 135: 234–243

Garcia-Guinea J, Townsend PD, Sanchez-Muoz L, Rojo JM (1999) Ultraviolet-blue ionic luminescence of alkali feldspars from bulk and interfaces. Phys Chem Miner 26: 658–667

Geake JE, Walker G (1975) Luminescence of minerals in the near-infrared. In: Karr C (ed) Infrared and Raman spectroscopy of lunar and terrestrial minerals. Academic Press, New York, pp 73–89

Götze J, Habermann D, Neuser RD, Richter DK (1999) High-resolution spectrometric analysis of REE-activated cathodoluminescence (CL) in feldspar minerals. Chem Geol 153: 81–91

Götze J, Krbetschek MR, Habermann D, Wolf D (2000) High-resolution cathodoluminescence studies of feldspar minerals. In: Pagel M, Barbin V, Blanc P, Ohnenstetter D (eds) Cathodoluminescence in geosciences. Springer, Berlin Heidelberg New York, pp 245–270

Habermann D (2002) Quantitative cathodoluminescence (CL) spectroscopy of minerals: possibilities and limitations. Mineral, Petrol, 76: 247–259

Harlow GE, Brown GE (1980) Low albite: an X-ray and neutron diffraction study. Am Mineral 65 986–995

Hobbs AN (1999) Dislocations in plagioclase feldspar. unpublished MPhil Thesis, University of Hertfordshire, UK

Homman NPO, Yang C, Malmqvist KG, Hanghøj K (1995) Plagioclase studies by ionoluminescence (IL) and particle-induced X-ray Emission (PIXE) employing a nuclear microprobe. Scanning Microscopy Supplement, 9: 157–165, Scanning Microscopy International, Chicago, USA

Krbetschek MR, Götze J, Irmer G, Rieser U, Trautmann T (2002) The red luminescence emission of feldspar and its wavelength dependence on K,Na,Ca composition. Mineral Petrol 76: 167–177

Parsons I (1979) The Klokken Gabbro-syenite complex, south Greenland: cryptic variation and origin of inversely graded layering. J Petrol 20: 653–694

Parsons I (1981) The Klokken Gabbro-syenite complex, south Greenland: quantitative interpretation of mineral chemistry. J Petrol 22: 233–260

Previtt CT, Sueno S, Papike JJ (1976) The crystal structures of high albite at high temperatures. Am Mineral 61: 1213–1225

Rae DA, Chambers AD (1988) Metasomatism in the North Qôroq centre, South Greenland: cathodoluminescence and mineral chemistry of alkali feldspars. Trans Roy Soc Edinburgh 79: 1–12

Smith JV, Artioli G (1986) Low albite, $NaAlSi_3O_8$: neutron diffraction study of the crystal structure at 13 K. Am Mineral 71: 727–733

Smith JV, Stenstrom RC (1965) Electron-excited luminescence as a petrologic tool. J Geol 73: 627–635

Telfer DJ, Walker G (1978) Ligand field bands of Mn^{2+} and Fe^{3+} luminescence centres and their site occupancy in plagioclase feldspars. Modern Geol 6: 199–210

Upton BGJ, Emeleus CH (1987) Mid-Proterozoic alkaline magmatism in Southern Greenland: the Gardar Province. In: Fitton JG, Upton BGJ (eds) Alkaline igneous rocks. Special Publication, Geological Society London 30: 449–471

Upton BGJ, Emeleus CH, Heaman LM, Goodenough KM, Finch AA (2003) The Gardar province: repeated rifting events in the mid-Proterozoic, South Greenland. Lithos (In press)

White WB, Masako M, Linneham DG, Furukawa T, Chandrasekhar BK (1986) Absorption and luminescence of Fe^{3+} in single crystal orthoclase. Am Mineral 71: 1415–1419

View publication stats